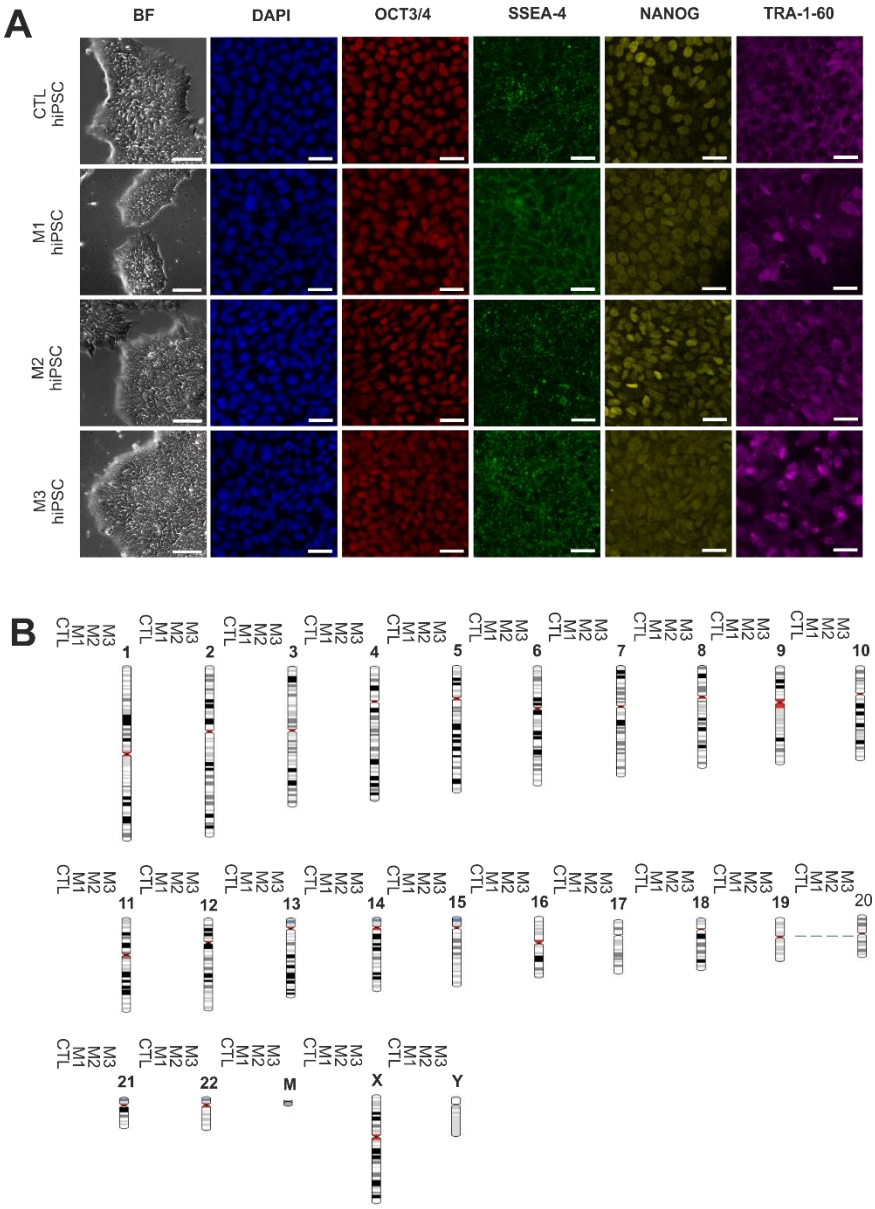

Fig. S1. Pluripotency immunocytochemistry and single nucleotide polymorphism (SNP)-karyotyping of CTL and *NF1*-mutant hiPSCs

A Brightfield (BF) images and immunocytochemical analysis of CTL and *NF1*-mutant hiPSC cells for OCT3/4, SSEA-4, NANOG and TRA-160 pluripotency markers. Scale bars, 100 μm (BF) and 30 μm.

B Virtual karyotype generated through SNP-karyotyping for all hiPSC lines. Areas of gain are marked in green, areas of loss in red, and loss of heterozygosity in gray.

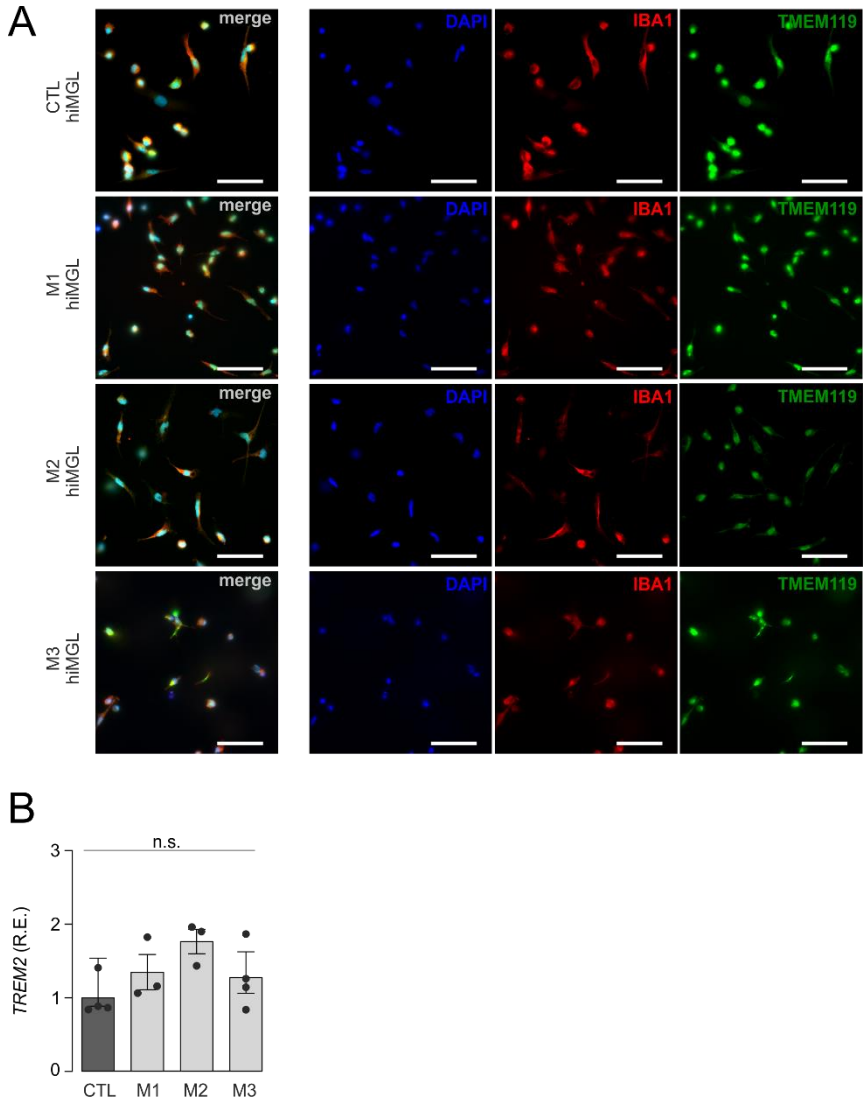

Fig. S2. Immunohistochemical staining and TREM2 expression in CTL and *NF1*-mutant hiMGL cells

A CTL and *NF1*-mutant hiMGL cells labelled with DAPI are immunopositive for IBA1 and TMEM119 expression. Merged images show the combined signal for DAPI, IBA1 and TMEM119. Scale bars, 50 μm.

B Relative mRNA expression levels of the *TREM2* microglia marker were assessed in CTL and *NF1*-mutant hiMGL cells by quantitative RT-qPCR. Relative expression (R.E.) was normalized relative to the TATA box binding protein (*TBP*) housekeeping gene (n=3). Results are represented as the mean ± SEM. Data were analyzed by one-way ANOVA followed by Tukey's multiple comparisons test.

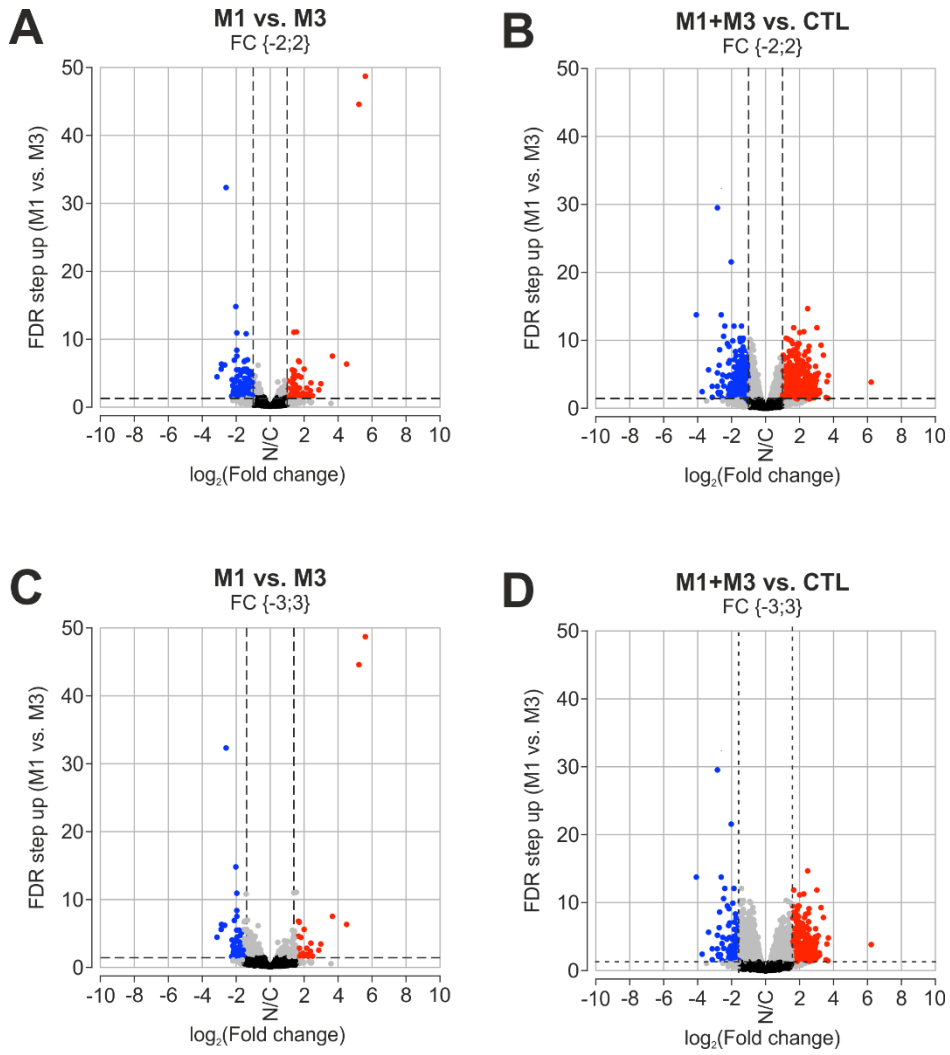

Fig. S3. RNAseq reveals few differences between NF1-mutant and CTL hiMGL cells

A Volcano plot demonstrating genes differentially expressed between M1 versus M3 [FDR < .05; fold change (-2, 2)]. Grey dots (no change), blue dots (decreased expression), red dots (increased expression

B Volcano plot demonstrating genes differentially expressed between M1 and M3 versus CTL [FDR < .05; fold change (-2, 2)]. Grey dots (no change), blue dots (decreased expression), red dots (increased expression).

C Volcano plot demonstrating genes differentially expressed between M1 versus M3 [FDR < .05; fold change (-3, 3)]. Grey dots (no change), blue dots (decreased expression), red dots (increased expression).

D Volcano plot demonstrating genes differentially expressed between M1 and M3 versus CTL [FDR < .05; fold change (-3, 3)]. Grey dots (no change), blue dots (decreased expression), red dots (increased expression).

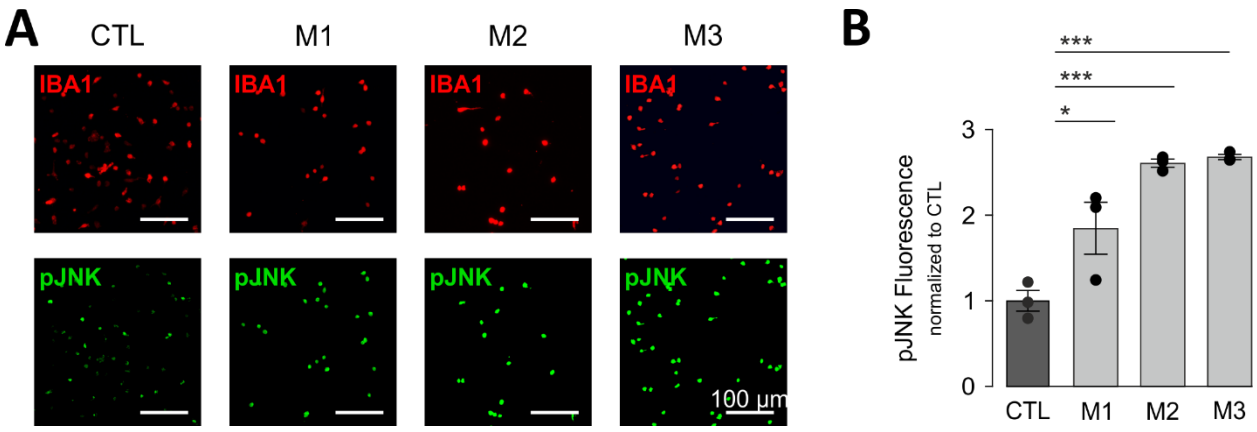

Fig. S4. *NF1*-mutant hiMGL cells show higher p-JNK expression than CTL hiMGL cells

A Immunohistochemical staining of CTL and *NF1*-mutant (M1-M3) hiMGL cells for IBA1 (red, *top*) and phosphorylated (activated) JNK (phospho-Thr^{183}/Tyr^{185} JNK, p-JNK; green, *bottom*). Scale bars, 100 µm.

B Quantification of phospho-JNK (p-JNK) fluorescence intensity in M1, M2 and M3 hiMGL cells, normalized to CTL hiMGL cells. Data indicated by asterisks were analyzed using a one-way ANOVA followed by Tukey's multiple comparisons test. *P<0.05; ***P<0.001. Results are represented as the mean +/- SEM. N = 3 independent differentiations for each mutant.

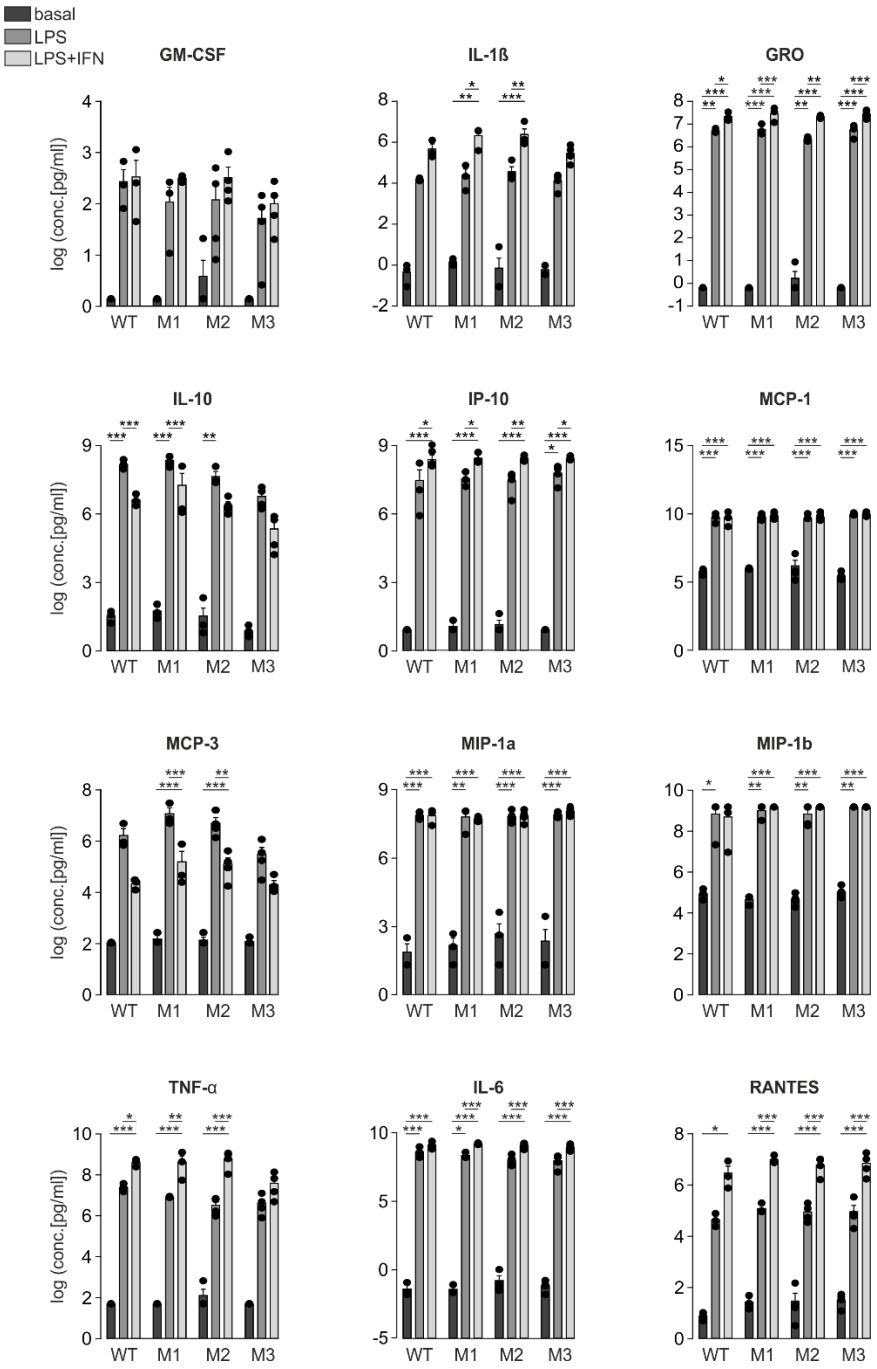

Fig. S5. Cytokine release from CTL and *NF1*-mutant hiMGL cells

A multiplex immunoassay was used to detect cytokines/chemokines secreted into the tissue culture medium by CTL and *NF1*-mutant hiMGL cells in response to stimulation with 1 µg/ml LPS or 1 µg/ml LPS + 100 ng/ml IFN-γ for 24h (n = 3-4). Data were analyzed by an ANOVA test. *P<0.05; **P< 0.01, ***P<0.001. Results are represented as the mean ± SEM.

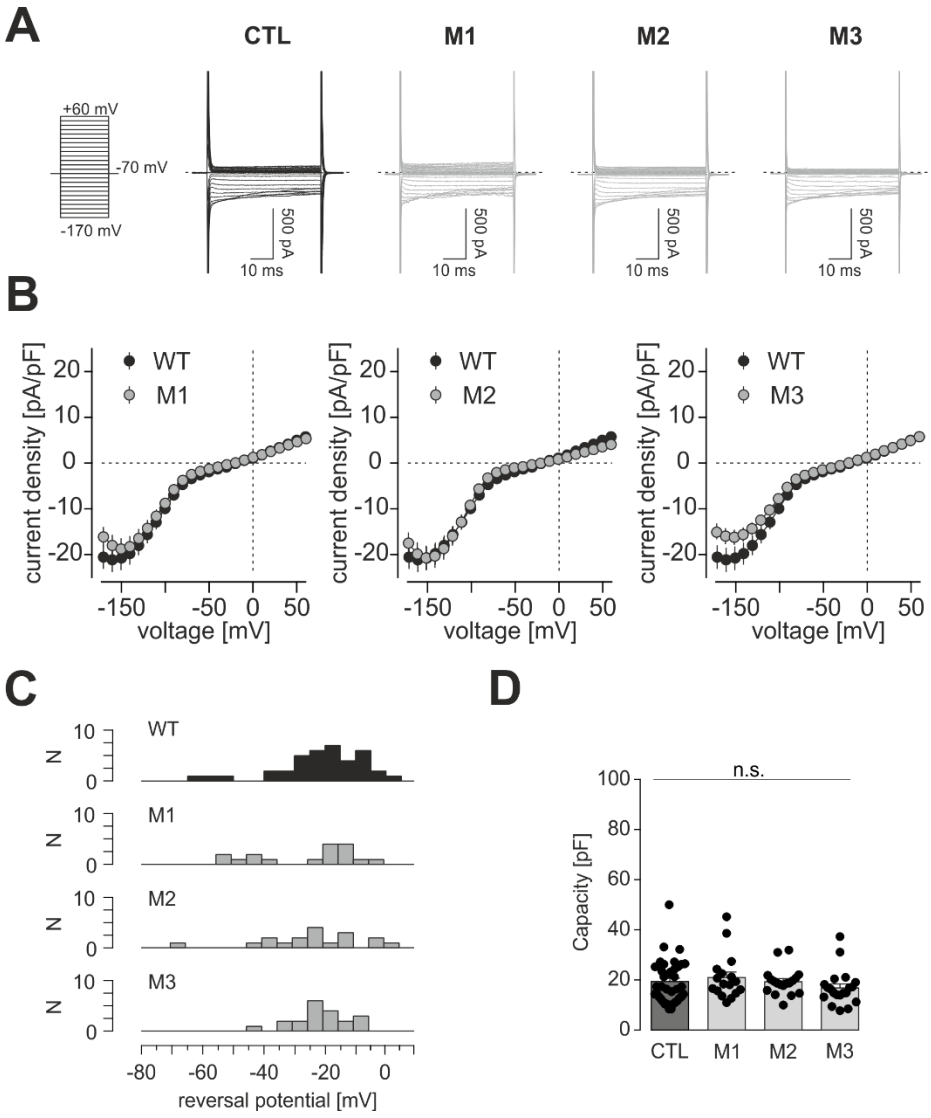

Fig. S6. Basal membrane properties of CTL and *NF1*-mutant hiMGL cells

A Sample patch clamp recordings of CTL and *NF1*-mutant hiMGL cells. Membrane currents were obtained during a series of voltage steps for 50 ms ranging from -170 mV to +60 mV from a holding potential of -70 mV.

B Average current density-voltage relationships of hiMGL cells obtained from the recordings shown in **A**.

C Distribution of the reversal potentials (indicative of the membrane potentials). N: number of patched cells.

D: Summary of the membrane capacities of CTL and *NF1*-mutant hiMGL cells.

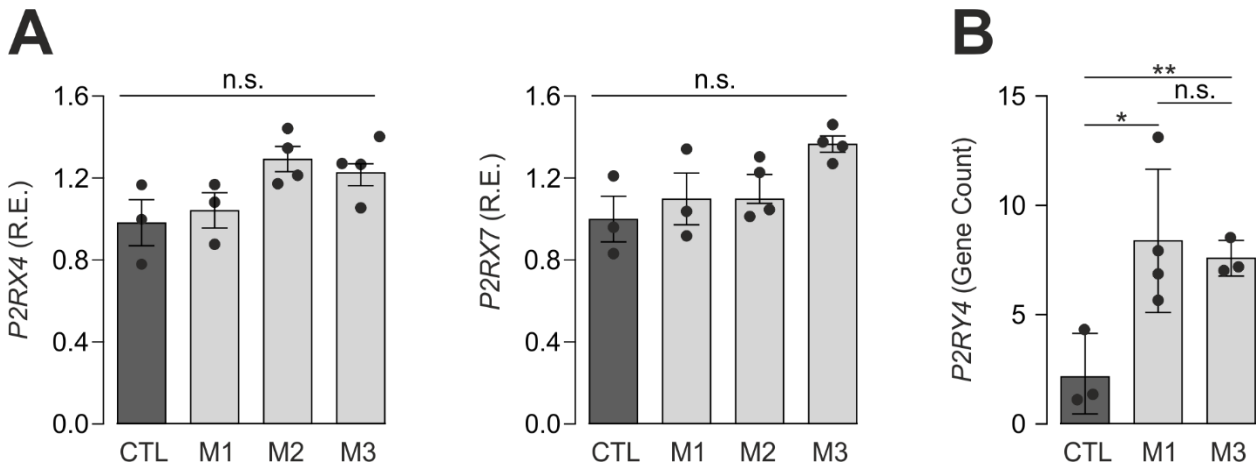

Fig. S7. Expression of P2RX4 and P2RX7 in CTL and *NF1*-mutant hiMGL cells

A: Relative *P2RX4* (left) and *P2RX7* mRNA expression (right) levels in CTL and *NF1*-mutant hiMGL cells by quantitative RT-PCR. TATA box binding protein (*TBP*) was used as a housekeeping gene for normalization (n = 3). Data were then normalized to mRNA expression levels in CTL hiMGL cells. Results are represented as the mean ± SD. Data were analyzed by one-way ANOVA.

B: P2 receptor expression from the RNA sequencing data revealed that only *P2RY4* expression was different in *NF1*-mutant hiMGL cells relative to CTL hiMGL cells. P values are included in the graph. All other genes were not statistically different between *NF1*-mutant and CTL hiMGL cell groups.

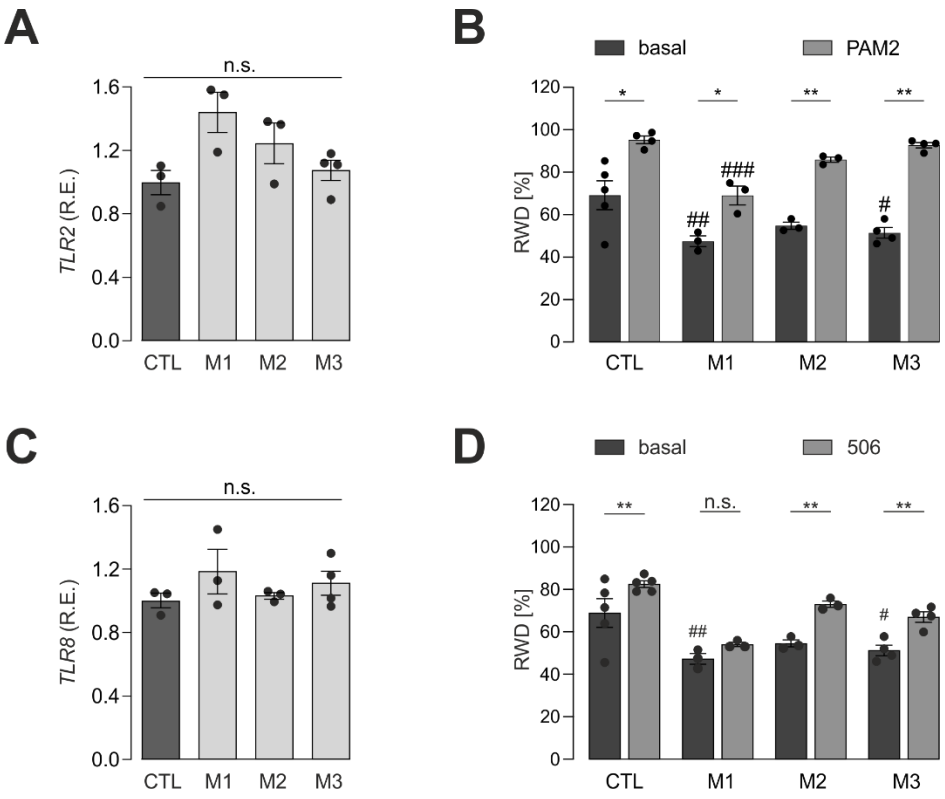

Fig. S8. Motility of CTL and *NF1*-mutant hiMGL cells

A Relative mRNA expression levels of Toll-like receptor 2 (*TLR2*) in CTL and *NF1*-mutant hiMGL cells by quantitative RT-PCR. Relative expression (R.E.) is shown relative to CTL hiMGL cells. TATA box binding protein (*TBP*) mRNA expression was used as a housekeeping gene for normalization (n = 3). Data were then normalized to *TLR2* expression of CTL hiMGL cells. Results are represented as the mean ± SEM. Data were analyzed by one-way ANOVA.

B Motility was assessed using a standardized wound scratch assay (RWD) using an Incucyte Zoom System. hiMGL cells were incubated with or without Pam2CSK4 (100 ng/ml). Relative Wound Density (RWD) was assessed over the course of two days comparing CTL and *NF1*-mutant hiMGL cells. Results are represented as the mean ± SEM. N = 5 for CTL and N = 3-4 for *NF1*-mutant hiMGL cells. Data indicated by the asterisks were analyzed by one-way ANOVA followed by Tukey's multiple comparisons test. *P<0.05; **P< 0.01, ***P<0.001. Comparisons between basal and Pam2CSK4 conditions were performed using a Student's t-test: #P<0.05, ###P<0.001.

C Relative mRNA expression levels of Toll-like receptor 8 (*TLR8*) was assessed in CTL and *NF1*-mutant hiMGL cells by quantitative RT-PCR. TATA box binding protein (*TBP*) was used as a housekeeping gene for normalization (n=3). Data were then normalized to *TLR8* expression of CTL hiMGL cells. Results are represented as the mean ± SD. Data were analyzed by one-way ANOVA.

D RWD after 36h was represented as the mean ± SEM. N = 5 for CTL and N = 3 for *NF1*-mutant hiMGL cells. hiMGL cells were incubated with or without 506 (100 ng/ml). Data indicated by the asterisks were analyzed by one-way ANOVA followed by Tukey's multiple comparisons test. *P<0.05; **P< 0.01, ***P<0.001. Comparisons between basal and 506 conditions were performed using a Student's t-test: ##P<0.01.

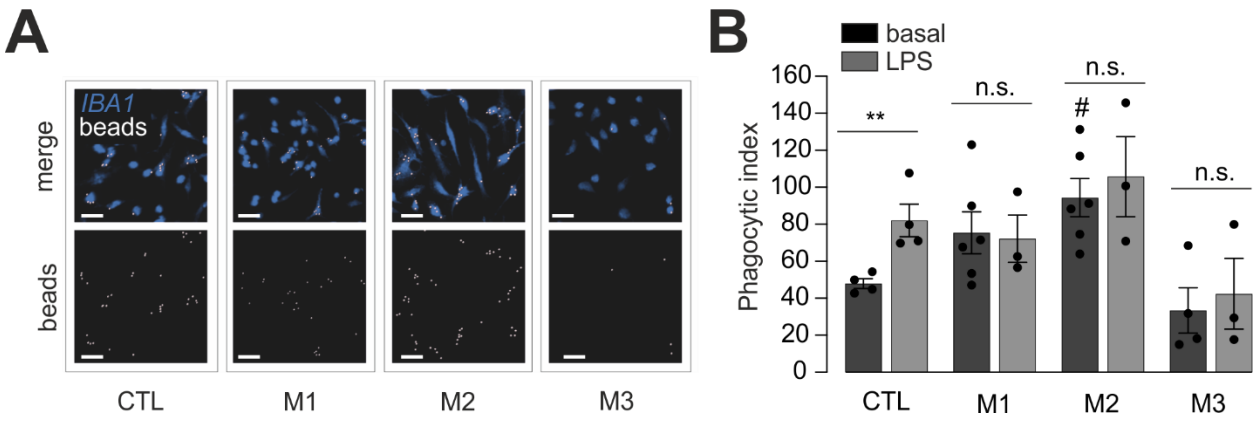

Fig. S9. Phagocytic activity of CTL and *NF1*-mutant hiMGL cells

Phagocytic activity was assessed by microscopy using fluorescent microbeads. CTL and *NF1*-mutant hiMGL cells were incubated for 1h with beads with or without addition of 1 µg/ml LPS.

A: Representative images of CTL and *NF1*-mutant hiMGL cells at the end of the assay period under LPS stimulation conditions. IBA1 staining is indicated in blue and beads in white. Scale bars, 20 µm.

B: Phagocytic activity presented as the phagocytic index, which is a measure of the percentage of cells harboring 0, 1, 2 or >3 engulfed beads. Data indicated by asterisks were analyzed by one-way ANOVA followed by Tukey's multiple comparisons test. *P<0.05; **P< 0.01, ***P<0.001. Comparisons between basal and UDP conditions were performed using a Student's t-test: ###P<0.001. Results are represented as the mean ± SEM. N = 5 for CTL and n = 3 for *NF1*-mutant hiMGL cells.

Table S1. Antibodies used

Antibody	Company	Host species	Dilution	Catalog number
Anti-IBA1	Abcam	Goat	1:250	ab5076
Anti-NANOG	Thermo Fisher Scientific	Rabbit	1:100	PA1-097
Anti Phospho-JNK (phospho-T183/Y185)	R&D Systems	Rabbit	1:100	MAB1205
Anti-OCT-3/4	Santa Cruz	Rabbit	1:100	sc-9081
Anti-P2RY12	Genetex	Rabbit	1:200	GTX54796
Anti-SSEA-4	Abcam	Mouse	1:100	ab16287
Anti-TMEM119	Abcam	Rabbit	1:200	ab185333
Anti-TRA-1-60	Abcam	Mouse	1:100	ab16288
Anti-Goat-AF488	Dianova	Donkey	1:200	705-545-147
Anti-mouse-AF647	Dianova	Donkey	1:125	715-605-151
Anti-rabbit-AF647	Dianova	Donkey	1:200	711-605-152
Anti-Goat-AF647	Dianova	Donkey	1:200	705-605-147

Table S2. Primers used

Primer		Sequence
AIF1	forward	5’- TTGGTGAGAAACGGGTGATTTG-3’
	reverse	5’- ATGGAGCATGTAGGAGAGACC-3’
P2RX4	forward	5’- GAGATTCCAGATGCGACCACT-3’
	reverse	5’- ACCCGTTGAAAGCTACGCAC-3’
P2RX7	forward	5’- TATGAGACGAACAAAGTCACTCG-3’
	reverse	5’- GCAAAGCAAACGTAGGAAAAGAT-3’
P2RY6	forward	5’- GTGTCTACCGCGAGAACTTCA-3’
	reverse	5’- CCAGAGCAAGGTTTAGGGTGTA-3’
P2RY12	forward	5’- CACTGCTCTACACTGTCCTGT-3’
	reverse	5’- AGTGGTCCTGTTCCCAGTTTG-3’
TBP1	forward	5’- AGCGCAAGGGTTTCTGGTTT-3’
	reverse	5’- CTGAATAGGCTGTGGGGTCA-3’
TLR2	forward	5’- TTATCCAGCACACGAATACACAG-3’
	reverse	5’- AGGCATCTGGTAGAGTCATCAA-3’
TLR4	forward	5’- TGGAAGTTGAACGAATGGAATGTG-3’
	reverse	5’- ACCAGAACTGCTACAACAGATACT-3’
TLR8	forward	5’- CCACCTTGAAGAGAGCCGAG-3’
	reverse	5’- TGCTCTGCATGAGGTTGTCG-3’
TMEM119	forward	5’- GAGGAGGGACGGGAGGAG-3’
	reverse	5’- CAGAAGGATGAGGAGGCTGG-3’

Table S3. Differentially expressed genes between M1 & M3 relative to CTL hiMGL cells

Gene name	P-value	FDR	Fold change (M1 & M3 vs. CTL)
DCANP1	6.18E-06	1.82E-04	71.76
GPR22	2.13E-05	4.53E-04	15.36
FOXN3-AS2	3.54E-10	1.07E-07	12.56
EHF	7.92E-05	1.18E-03	9.39
SAA1	7.42E-04	6.31E-03	9.31
YY1P1	5.45E-12	3.98E-09	9.00
RNF43	3.96E-03	2.18E-02	8.81
KCNAB1	2.76E-06	1.00E-04	7.57
ZNF22-AS1	2.83E-05	5.54E-04	7.44
CDH1	8.37E-04	6.93E-03	7.18
DSP	7.36E-05	1.12E-03	7.01
FAM83B	1.49E-03	1.06E-02	6.99
TAS2R30	5.23E-05	8.71E-04	6.65
OR7E38P	7.98E-06	2.17E-04	6.56
GAS8	6.93E-03	3.28E-02	6.54
KLB	2.36E-03	1.47E-02	6.36
OGN	1.29E-07	1.00E-05	6.32
EIF1P7	7.56E-03	3.51E-02	6.11
PLGLB2	6.39E-07	3.33E-05	6.02
LBH	1.08E-03	8.39E-03	5.95
PLN	2.00E-05	4.35E-04	5.94
LAMP3	9.26E-04	7.43E-03	5.90
PRMT5-AS1	7.23E-04	6.20E-03	5.76
SRGAP2-AS1	1.77E-05	3.99E-04	5.70
GNPDA2	3.21E-07	1.97E-05	5.45
PIGAP1	1.63E-06	6.66E-05	5.23
TAS2R13	4.79E-05	8.22E-04	5.22
DIAPH1-AS1	4.10E-09	7.42E-07	5.21
HSBP1L1	7.00E-03	3.30E-02	5.18
CCL22	7.69E-05	1.16E-03	5.18
CTXND1	8.63E-03	3.87E-02	5.16
CD1A	1.19E-08	1.68E-06	5.16
ATP5PDP4	2.24E-06	8.42E-05	5.13
TAS2R31	5.12E-04	4.81E-03	5.12
OR10A2	6.28E-04	5.59E-03	5.09
MANEA-DT	5.40E-03	2.72E-02	5.08
HSPD1P11	1.56E-03	1.09E-02	5.02
TMEM178A	1.61E-03	1.12E-02	-5.20
SAP25	2.52E-18	9.56E-15	-5.28
DNAH8	3.41E-04	3.57E-03	-5.39
PDCD6-AHRR	1.73E-14	4.11E-11	-5.80

TNFSF9	3.42E-06	1.18E-04	-5.94
SYNPO2L-AS1	6.61E-08	6.03E-06	-5.94
CAT	1.70E-20	1.08E-16	-6.39
DNAAF4-CCPG1	6.59E-06	1.90E-04	-6.39
GOPC	7.45E-27	1.21E-22	-6.90
MUSTN1	5.03E-04	4.77E-03	-7.80
CEMP1	7.07E-07	3.59E-05	-8.05
SDHAP2	6.63E-13	7.51E-10	-15.60

Table S4. Differentially expressed genes between M1 vs. M3 hiMGL cells

Gene name	P-value	FDR	Fold change (M1 vs. M3)
GOPC	7.08E-40	1.35E-35	46.33
ZNF252P	2.21E-33	2.10E-29	30.69
DNAAF4-CCPG1	6.18E-05	1.07E-02	10.40
MIR124-1HG	2.11E-04	2.39E-02	5.18
PCDHA10	3.09E-04	3.14E-02	5.04
BIRC3	2.29E-04	2.50E-02	-5.08
LTBP1	2.67E-08	2.21E-05	-5.96
PCDHGA10	1.66E-28	1.05E-24	-6.03
PRSS8	2.14E-09	2.55E-06	-6.69
TSSC2	4.48E-05	8.60E-03	-9.57
EHF	3.19E-11	5.05E-08	-11.10

Table S5. Materials for cell culture and *in vitro* experiments

Product name	Company	Catalog number
α-Thioglycerol	Merck	M1753-100ML
24-well plates	Sarstedt	83.3922
4′,6-diamidino-2-phenylindole (DAPI)	Merck	32670
Aqua-Poly/Mount	Polysciences Europe GmbH	18606
B-27 Supplement (50X), serum free	Life Technologies	17504-044
Bambanker	GC Lymphotec	302-14681
CD200, Human 50µg	Novoprotein	C311
CX3CL1, 5µg	Peprotech	300-31
Cyclic CAMP ELISA Kit	Cayman Chemical	581001
DMEM/F-12, HEPES, no phenol red	Life Technologies	11039-021
Donkey serum	Merck	S30
Falcon® 6-well Clear Flat Bottom Plates	Corning	353046
Fetal Calf Serum (FCS)	Life Technologies	10270-106
Fluoresbrite® YG Carboxylate Microspheres, 3.00µm	Polysciences Europe GmbH	17147-5
Geltrex™	Life Technologies	A14133-02
GlutaMAX Supplement-100 mL	Life Technologies	35050-038
HBSS	Life Technologies	14175-129
Human Insulin	PromoCell	C-52310
IL-34 2µg	Peprotech	200-34
Incucyte® Imagelock 96-well plates	Sartorius	BA-04856
Insulin-Transferrin-Selenite	Life Technologies	41400-045
Lipopolysaccharide from *E.coli*	Merck	L43191
M-CSF	Peprotech	300-25
MEM Non-Essential Amino Acids Solution (100X)-100 mL	Life Technologies	11140-035
TLR2 Agonist Pam2CSK4	R&D Systems	4637/1
P2RX4 Inhibitor 5-BDBD	R&D Systems	3579/10
P2RX7 Inhibitor A 740003	Tocris	3701
P2RY12 Inhibitor ARC-69931 Tetrasodium salt	Tocris, Bio-Techne GmbH	5720/1
N-2 Supplement (100X)	Life Technologies	17502-048
PBS	Life Technologies	14190-169
ReliaPrep™ RNA Tissue Kit	Promega	Z6112
STEMdiff™ Hematopoietic Kit	Stemcell Technologies	5310
StemMACS™ iPS-Brew XF	Miltenyi Biotec	130-107-086
StemPro® Accutase®	Life Technologies	A11105-01
SYBR Green Master Mix	Life Technologies	4472918
TGFβ1	Peprotech	100-21C
TL8-506	InvivoGen	Tlrl-Tl8506
Thiazovivin	StemCell Technologies™	72252
Triton® X-100	Roth	3051.3